J. Cent. South Univ. (2018) 25: 490−498
DOI: https://doi.org/10.1007/s11771-018-3753-4

Springer

Microstructural evolution of 2026 aluminum alloy during homogenization

JIANG Ding-bang(蒋鼎邦)[1], PAN Qing-lin(潘清林)[1], HUANG Zhi-qi(黄志其)[2], HU Quan(胡权)[2], LIU Zhi-ming(刘志铭)[2]

1. School of Materials Science and Engineering, Central South University, Changsha 410083, China;
2. Guangdong Fenglv Aluminum Company Ltd, Foshan 528133, China

Abstract: The microstructural evolution of 2026 aluminum alloy during homogenization treatment was investigated by optical microscopy (OM), scanning electron microscopy (SEM), energy dispersive X-ray spectrometry (EDS), differential scanning calorimetry (DSC) and X-ray diffraction (XRD). The results show that severe dendritic segregation exists in the as-cast 2026 alloy and the main secondary phases at grain boundary are S (Al_2CuMg) and θ (Al_2Cu) phases. Elements Cu, Mg and Mn distribute unevenly from grain boundary to the inside of as-cast alloy. With the increase of homogenization temperature or the prolongation of holding time, the residual phases gradually dissolve into the matrix α(Al) and all the elements become more homogenized. According to the results of microstructural evolution, differential scanning calorimetry and X-ray diffraction, the optimum homogenization parameter is at 490 °C for 24 h, which is consistent with the result of homogenization kinetic analysis.

Key words: 2026 aluminum alloy; dendritic segregation; homogenization; microstructure evolution; homogenization kinetics

Cite this article as: JIANG Ding-bang, PAN Qing-lin, HUANG Zhi-qi, HU Quan, LIU Zhi-ming. Microstructural evolution of 2026 aluminum alloy during homogenization [J]. Journal of Central South University, 2018, 25(3): 490–498. DOI: https://doi.org/10.1007/s11771-018-3753-4.

1 Introduction

The Al–Cu–Mg alloys are widely used in aerospace and transportation industries because of their high strength, good toughness and excellent properties [1–4]. In order to satisfy the demand for high-strength aluminum alloys and improve the safety of airplanes, ALCOA corporation developed a new Al–Cu–Mg alloy which was known as 2026 aluminum alloy in 2001 [5]. At the basis of the predecessor 2024 aluminum alloy, 2026 aluminum alloy containing less natural impurities (Fe and Si), and the addition of zirconium strongly inhibits the recrystallization during thermo-mechanical processing [6, 7]. Therefore, 2026 aluminum alloy exhibits excellent comprehensive properties, including high tensile strength, excellent fatigue resistance and fracture toughness [6–8].

The structures and mechanical performances of Al–Cu–Mg alloys are associated with the structure of as-cast alloys, heat treatment and subsequent deformation conditions [9, 10]. During casting process, the non-equilibrium eutectic structure and dendritic structure can be produced because of the rapid cooling and non-equilibrium crystallization. These factors weaken the workability of the cast structure and ultimately affect the mechanical properties of aluminum alloys [11–14]. Therefore, in order to obtain excellent mechanical properties and overall performances of alloys, homogenization heat treatment is a primary

Foundation item: Project(2016B090931001) supported by Science and Technology Research and Development Program of Guangdong Province, China
Received date: 2016−07−13; **Accepted date:** 2017−12−20
Corresponding author: PAN Qing-lin, PhD, Professor; Tel: +86–731–88830933; E-mail: pqlcsu@163.com; ORCID: 0000-0002-3951-6819

and important step before processing [13, 14]. Moreover, different variations of the homogenization temperature and homogenization time have a great influence on the dissolution of the non-equilibrium phase. SHI et al [15] studied the influence of homogenization treatment on microstructure of DC cast 7085 aluminum alloy. DENG et al [16] reported the intermetallic phase transformation of 7050 aluminum alloy during homogenization treatment. SHI et al [15] and DENG et al [16] acquired proper homogenization processing respectively which agrees with homogenizing kinetic analysis. LIU et al [17] examined the microstructure evolution of Mg, Ag and Zn micro-alloyed Al–3.8Cu–1.28Li alloy ingot during two-step homogenization.

In the last few years, a large number of researches concerned on 2026 aluminum alloy have been reported. GARRATT et al [18] investigated the grain boundary geometry for optimum resistance to growth of short fatigue cracks in 2026 aluminum alloy. LAM et al [7] studied the response of 2026 aluminum alloy subjected to tensile deformation. ZHANG et al [19, 20] reported the hot deformation behavior of 2026 aluminum alloy during compression. However, the homogenization treatment of 2026 aluminum alloy has been rarely studied.

The purpose of the present work is to investigate the effects of homogenization on microstructure evolution and composition distribution of 2026 aluminum alloy. The homogenization kinetic equation is established successfully. These results can provide indispensable information for optimizing the actual processing parameters.

2 Experiment

The 2026 aluminum alloy was produced by semi-continuous casting. The chemical composition of 2026 aluminum alloy was analyzed with inductively coupled plasma atomic emission spectrometry (ICP-AES) as shown in Table 1. Slices with dimensions of 10 mm×10 mm× 3 mm were cut from the half position between the center and the surface layer of as-cast ingot. The specimens were homogenized at 460, 470, 480, 490 and 500 °C for 24 h, respectively. And then the specimens were homogenized for 8, 16, 24 and 32 h at the optimized temperature. The temperature variation was controlled within ±2 °C. All the homogenized specimens were air-cooled to room temperature.

Table 1 Nominal composition of studied alloy(mass fraction, %)

Cu	Mg	Mn	Zr	Fe	Si	Al
3. 81	1. 30	0. 56	0. 11	0. 063	0. 067	Bal.

OM images were obtained with a Leica DMILM optical microscope. SEM observation with the backscatter electron image mode was carried out on a FEI Quanta-200 scanning electron microscope. The specimens for OM observation were prepared through a conventional mechanical grinding and polishing, followed by etching with Keller reagent. The map and line scanning analyses were conducted on an energy dispersive X-ray spectrometer (EDS, Genesis 60S) operated at 20 kV. Differential scanning calorimetry (DSC) analysis was carried out on an NETZSCH STA−449C equipment which purified argon atmosphere ranging from room temperature to 700 °C. X-ray diffraction (XRD) analysis was performed on a D/max 2500 PC diffractometer.

3 Results and discussion

3.1 As-cast microstructure

Figure 1 shows the microstructures of the as-cast alloy. A typical as-cast eutectic structure with severe dendrite segregation in Figure 1(a) requires further heat treatment to eliminate. Also, it should be noted that a considerable number of secondary phases exist at the grain boundaries. EDS results of the secondary phases in as-cast alloy are listed in Table 2. Combining with the EDS results, as shown in Figure 1(b), the point A is θ (Al_2Cu) phase which only contains elements Al and Cu while the grey phase shown at point B is the S (Al_2CuMg) phase [6, 7, 21].

Figure 2 presents the distribution of the main elements Al, Cu, Mg and Mn in as-cast alloy. The main elements Cu, Mg and Mn are largely enriched at grain boundaries, and the concentration of the elements decreases from grain boundary to inside. The differences in brightness show the segregation degree of alloy elements: Cu>Mg>Mn. As is well known, the segregation and component

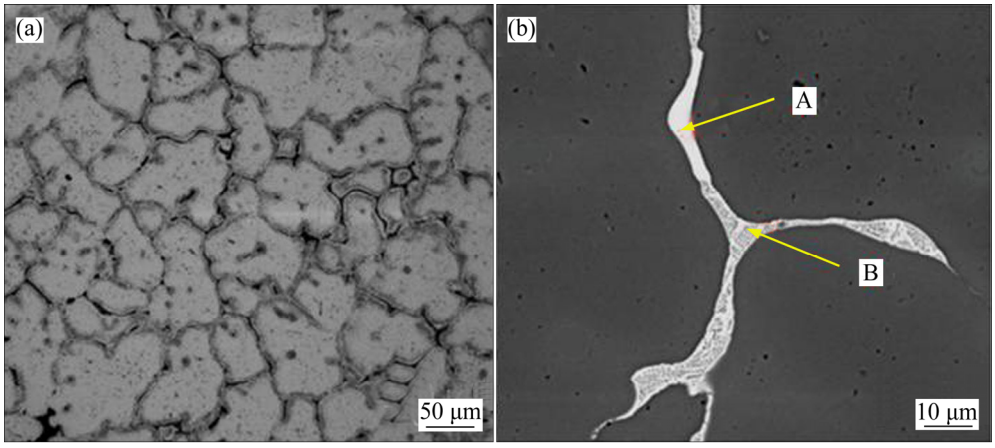

Figure 1 Microstructures of as-cast 2026 alloy: (a) OM image; (b) SEM image

Table 2 Chemical composition of the secondary phases in as-cast 2026 alloy shown in Figure 1(b) (mole fraction, %)

Point	Al	Cu	Mg
A	72. 02	27. 98	—
B	75. 66	17. 20	7. 14

inhomogeneity of as-cast alloy usually have hereditary influence on semi-products and finished products [15]. Therefore, the homogenization treatment is required to eliminate severe dendritic segregation in as-cast alloy. According to Refs. [9, 12], the homogenization treatment is related to the diffusion of atom. Generally, the relationship between the diffusion coefficient and the temperature can be expressed as

$$D = D_0 \exp\left(-\frac{Q}{RT}\right) \quad (1)$$

where D_0 is the diffusion coefficient; Q is the diffusion activation energy; R is the molar gas constant; T is the thermodynamic temperature. Based on Eq. (1), the higher the temperature is, the larger the diffusion coefficient will be. This makes it easier to eliminate the dendritic segregation in the as-cast alloy. However, the homogenization temperature should not exceed overburnt temperature of 2026 aluminum alloy. Therefore, it is highly necessary to obtain the optimum parameters of homogenization.

3.2 DSC and XRD analyses

DSC curves of as-cast and homogenized 2026 aluminum alloy are shown in Figure 3. Two endothermic peaks are observed in the as-cast alloy, sited at 510.1 °C and 643.5 °C, respectively. The endothermic peak at 510.1 °C gradually disappears with the increase of homogenization temperature, which may correspond to the dissolution of some non-equilibrium phases during homogenization. The endothermic peak at 643.5 °C is ascribed to the melting point of 2026 aluminum alloy. The results indicate that the upper limit temperature for homogenization of the 2026 aluminum alloy is 510.1 °C, which is generally termed the overburnt temperature.

Figure 4 shows the XRD patterns of 2026 aluminum alloy. The S (Al_2CuMg) and θ (Al_2Cu) phases are distinguished from XRD result in the as-cast alloy. With the increase of homogenization temperature, the diffraction peaks of S and θ phases decrease gradually and disappear eventually at 480 °C for 24 h. This may be due to the fact that the contents of S and θ phases in the matrix α (Al) are too low so that the detection is difficult by XRD. Therefore, when the homogenization temperature increases to 490 °C, there are no other obvious diffraction peaks in the XRD patterns except for matrix α. In other words, most of S and θ phases are dissolved into the matrix α.

3.3 Effect of homogenization temperature on microstructures

Figure 5 shows the SEM microstructures of specimens homogenized at different temperatures for 24 h. It suggests that the microstructure of 2026 aluminum alloy is determined by the homogenization temperature. With the increase of the homogenization temperature, the volume fraction of the residual phases is significantly decreased, and the continuous residual phases along

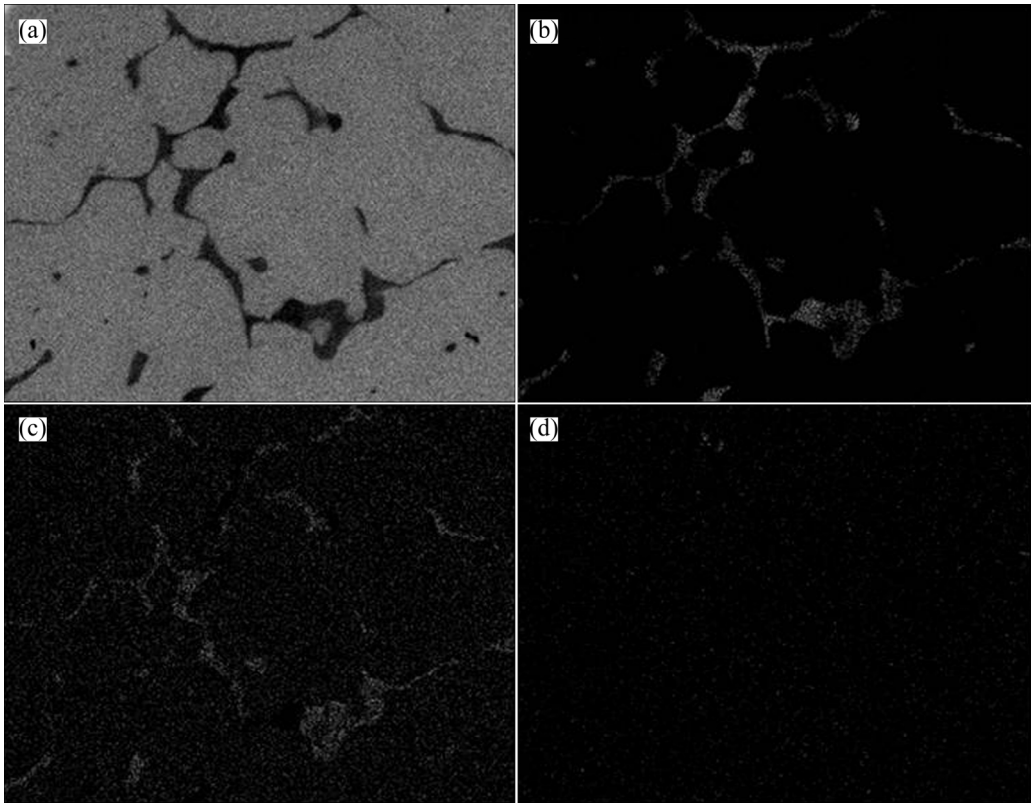

Figure 2 Elements distribution of Al (a), Cu (b), Mg (c) and Mn (d) in as-cast alloy

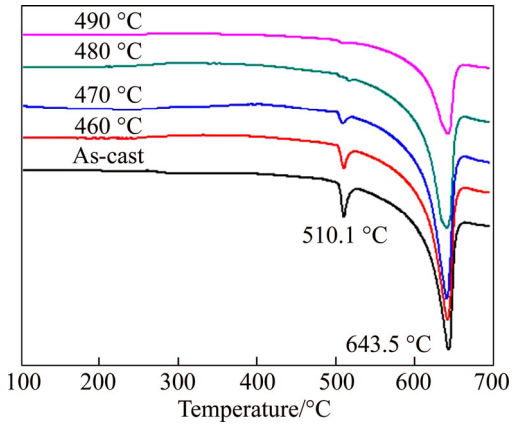

Figure 3 DSC curves of as-cast and homogenized alloy

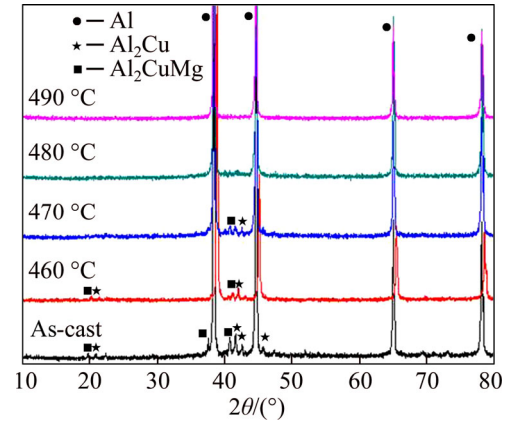

Figure 4 XRD patterns of as-cast and homogenized alloy

grain boundaries become discontinuous. At the same time, the grain boundaries become thinner and clearer (Figures 5(a)–(c)). When the specimen is homogenized at 490 °C for 24 h, the dendritic network structure reduces and most residual phases are spread homogeneously in matrix α(Al) (Figure 5(d)). However, when the homogenization temperature is 500 °C, a small amount of the melting compounds and redissolved triangular constituents at the grain boundaries can be observed, indicating that the specimen is overburnt (Figure 5(e)). According to the microstructure evolution, the appropriate homogenization temperature is 490 °C, consistent with the DSC curves in Figure 3 and XRD patterns in Figure 4.

3.4 Effect of homogenization time on microstructures

Figure 6 gives the SEM and optical images of specimens homogenized at 490 °C for different time. With prolonging the homogenization time, the volume fraction of dendritic network structure gradually decreases, the residual phases at the grain boundaries dissolve gradually. At the same time, the residual phases become small and sparse.

When homogenization time increases to 24 h,

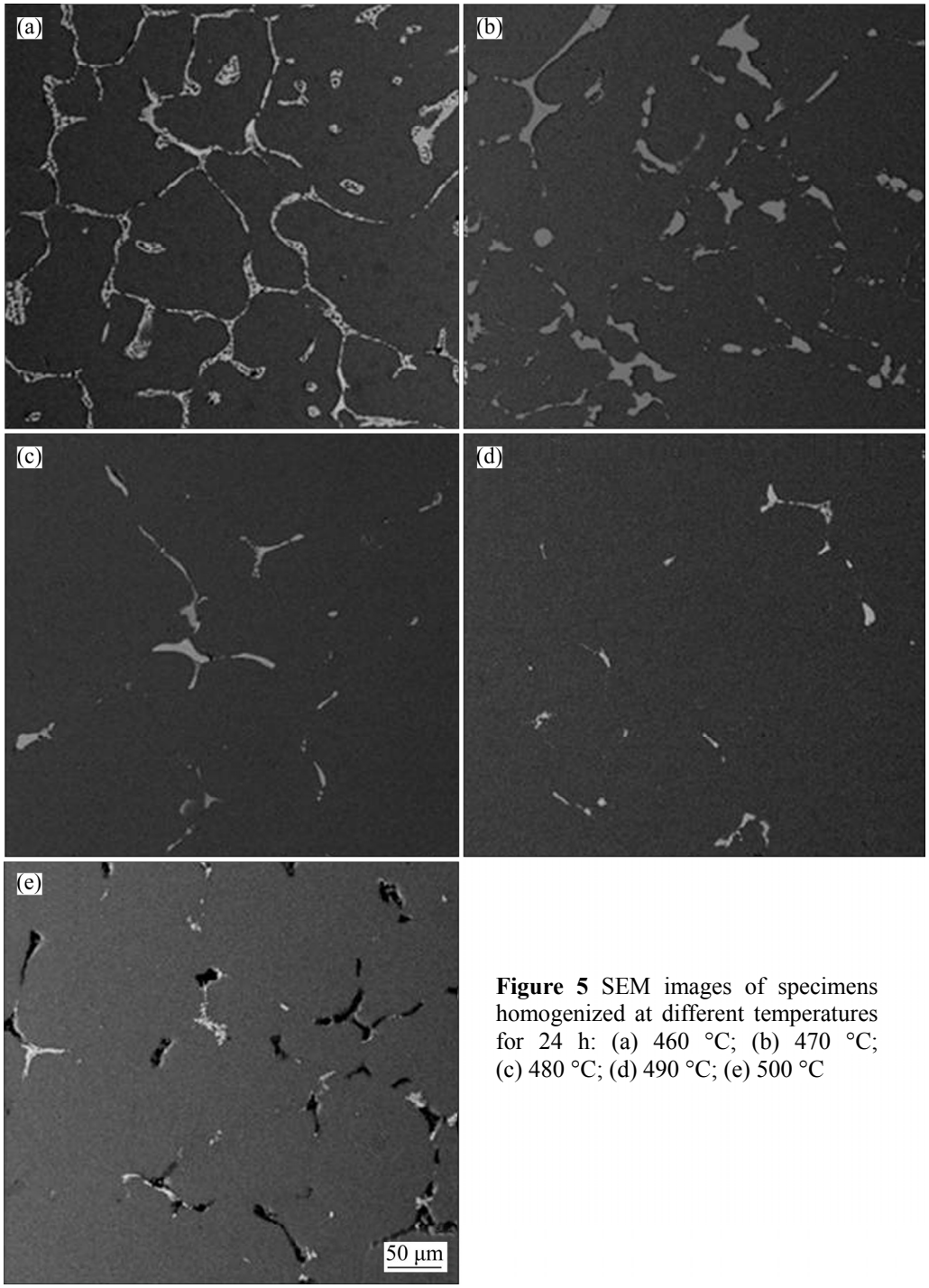

Figure 5 SEM images of specimens homogenized at different temperatures for 24 h: (a) 460 °C; (b) 470 °C; (c) 480 °C; (d) 490 °C; (e) 500 °C

the residual phases are almost dissolved into the matrix α (Al) (Figures 6(e)–(f)). When specimen is homogenized for 32 h, no significant dissolution of residual constituents is observed (Figures 6(g)–(h)), and the microstructure has no obvious change compared with that homogenized for 24 h. Table 3 lists the EDS results of the specimens homogenized at 490 °C for 24 h and 32 h. Point A shows that the residual phase contains 79.37% Al, 10.27% Cu, 6.94% Mn and 3.42% Fe (mole fraction) and Point B shows that the residual phase contains 75.32% Al, 15.36% Cu, 5.45% Mn and 3.87% Fe (mole fraction), which indicate that the residual phases may belong to $Al_{20}Cu_6(FeMn)_3$ phases. $Al_{20}Cu_6(FeMn)_3$ phase is an indissolvable impurity phase in the Al–Cu–Mg alloys, and difficult to be completely eliminated by homogenization treatment [6, 7]. Therefore, the optimum homogenization process of 2026 aluminum alloy is at 490 °C for 24 h.

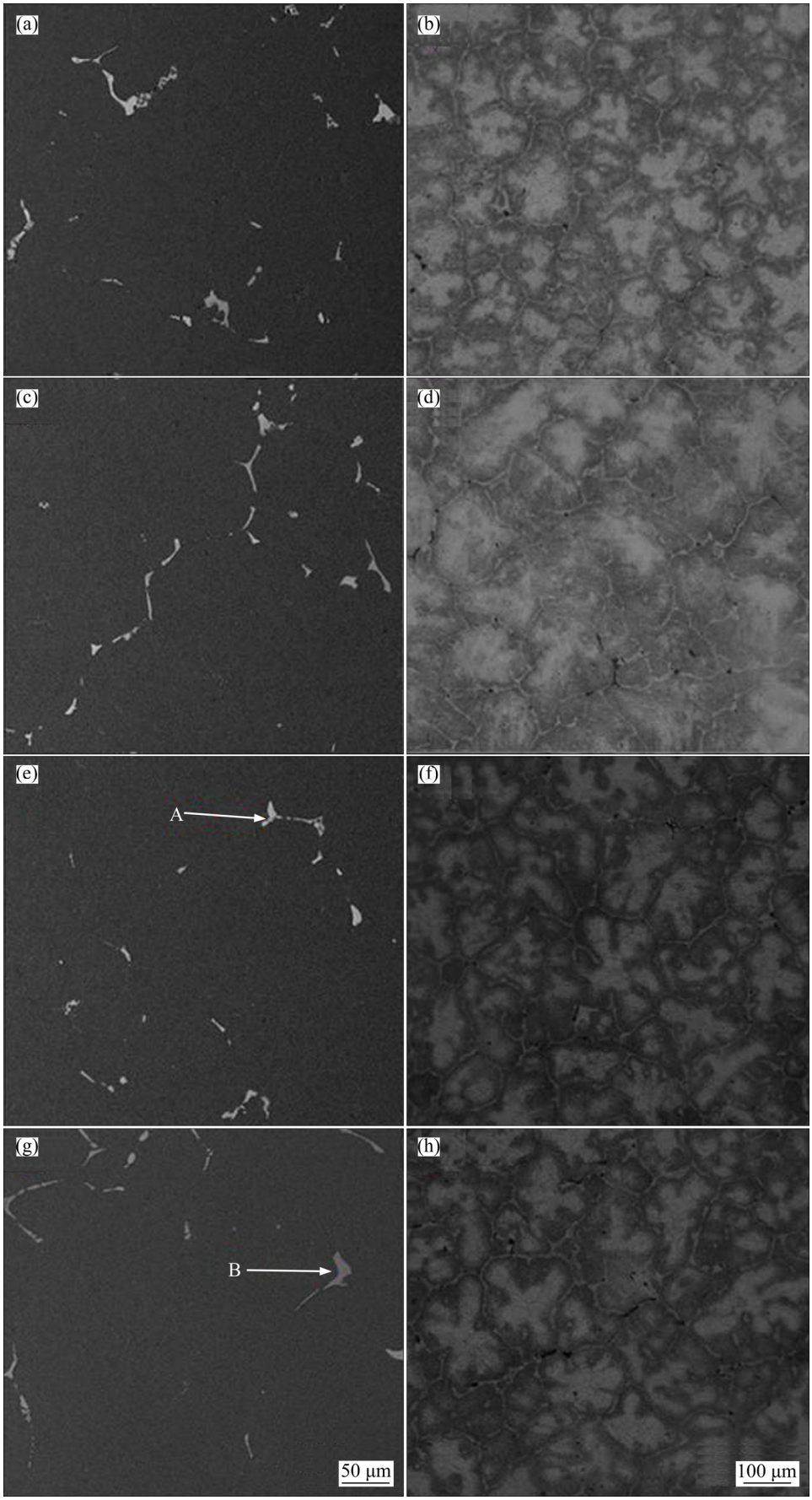

Figure 6 SEM images (a, c, e, g) and optical images (b, d, f, h) of specimens homogenized at 490 °C for different time: (a, b) 8 h; (c, d) 16 h; (e, f) 24 h; (g, h) 32 h

Table 3 Chemical composition of 2026 alloy shown in Figures 6(e)–(g) (mole fraction, %)

Point	Al	Cu	Mg	Mn	Fe
A	79.37	10.27	—	6.94	3.42
B	75.32	15.36	—	5.45	3.87

3.5 Line scanning and homogenization kinetic analysis

Figure 7 shows the line scanning analysis of as-cast 2026 alloy. Main elements Cu, Mg and Mn distribute unevenly from grain boundary to inside of the as-cast alloy. The studies of diffusion law along interdendritic region are important to the investigations of elements distribution during homogenization [14–16]. According to Refs. [9, 23], the initial concentration of the elements along the interdendritic region can be approached by Fourier series components in a cosine functions:

$$c(x)=\bar{c}+A_0\cos\left(\frac{2\pi x}{L}\right) \tag{2}$$

where $\bar{c}$ is the average concentration of the element; L is the interdendritic spacing; A_0 is the initial amplitude of composition segregation, which can be shown as

$$A_0=\frac{c_{\max}-c_{\min}}{2}=\frac{1}{2}\Delta c_0 \tag{3}$$

According to the second Fick's law and the boundary conditions [16], $A_{(t)}$ can be expressed as follows:

$$A_{(t)}=A_0\exp\left(-\frac{4\pi^2 Dt}{L^2}\right) \tag{4}$$

From Eq. (1) to Eq. (4), the equation can be rewritten as

$$A_{(t)}=A_0\exp\left[-\frac{4\pi^2 D_0 t}{L^2}\exp\left(-\frac{Q}{RT}\right)\right] \tag{5}$$

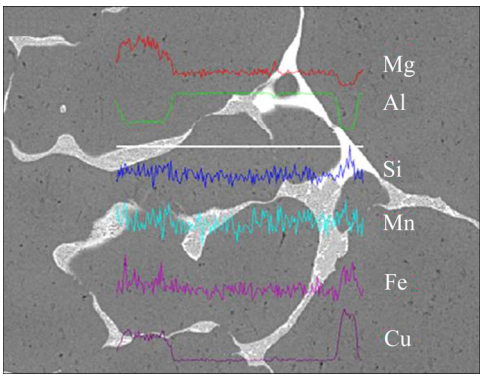

Figure 7 Line scanning analysis of as-cast 2026 alloy

where T is the homogenization temperature; t is the holding time. According to Eq. (5), with the increase of homogenization temperature T or the holding time t, the segregation along the interdendritic region decreases, which is consistent with the experimental result.

Assuming that the element distribution is homogeneous when the composition segregation amplitude is reduced to 1% [14, 24], that is

$$\exp\left[-\frac{4\pi^2 D_0 t}{L^2}\exp\left(-\frac{Q}{RT}\right)\right]=\frac{1}{100} \tag{6}$$

By taking natural logarithms of both sides, Eq. (6) can be rewritten as

$$\frac{1}{T}=\frac{R}{Q}\ln\left(\frac{4\pi^2 D_0 t}{4.6L^2}\right) \tag{7}$$

Equation (7) is the homogenization kinetic equation. If the parameters of as-cast microstructure are given, the homogenization kinetic curves can be obtained [13]. From previous Ref. [22], the diffusion coefficient of Cu is much lower than that of Mg or Mn at the same temperature. Thus, the homogenization process is considered to be controlled by the diffusion of Cu. The diffusion constant D_0 and diffusion activation energy Q of Cu in aluminum alloy are D_0(Cu)=0.084 cm^2/s and Q(Cu)=136.8 kJ/mol [14, 15]. According to the parameters, the homogenization kinetic curves of 2026 aluminum alloy for different interdendritic spacing can be fitted, as shown in Figure 8. It can be seen that with the increase of interdendritic spacing L, higher temperature and longer time are necessary for homogenization. Moreover, the time of homogenization reduces greatly with the increase of homogenization temperature.

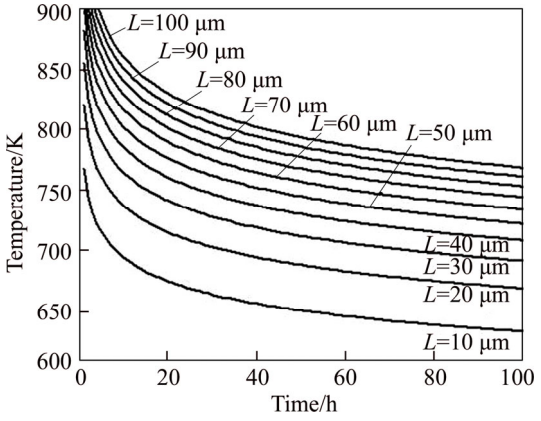

Figure 8 Homogenization kinetics curves of 2026 aluminum alloy

By substituting the average interdendritic spacing L into Eq. (7), suitable homogenizing parameters are obtained. Figure 9 shows the relationship between homogenization time and interdendritic spacing of aluminum alloy at 490 °C. On the basis of quantitative metallographic analysis, the average interdendritic spacing L of as-cast 2026 alloy is 49 μm. As seen in Figure 9, the corresponding homogenization time is 21.7 h. The calculated results agree well with the experimental results.

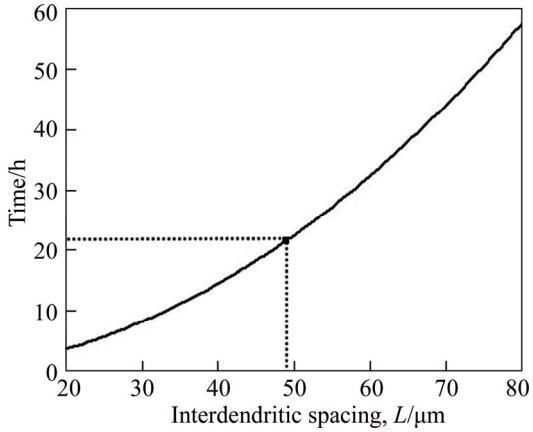

Figure 9 Relationship between homogenization time and interdendritic spacing of 2026 aluminum alloy at 490 °C

4 Conclusions

1) Serious dendritic segregation exists in as-cast 2026 alloy. The main secondary phases are θ (Al_2Cu) and S (Al_2CuMg) phases, which are distributed along grain boundaries. The main elements Cu, Mg and Mn distribute unevenly from grain boundary to the inside of as-cast alloy.

2) With the increase of homogenization temperature or the prolongation of holding time, the residual phases dissolve into the matrix gradually. Meanwhile, the grain boundaries become sparse and the distribution of all the elements becomes more homogenized. By taking experimental result and practical production into consideration, it is recommended that the suitable homogenization treatment is at 490 °C for 24 h.

References

[1] LI Li, LI Hui-zhong, LIANG Xiao-peng, HUANG Lan, HONG Tao. Flow stress behavior of high-purity Al-Cu-Mg alloy and microstructure evolution [J]. Journal of Central South University, 2015, 22(3): 815–820.

[2] WILLIAMS J C, STARKE E A. Progress in structural materials for aerospace systems [J]. Acta Materialia, 2003, 51(19): 5775–5799.

[3] LIU J Z, YANG S S, WANG S B, CHEN J H, WU C L. The influence of Cu/Mg atomic ratios on precipitation scenarios and mechanical properties of Al–Cu–Mg alloys [J]. Journal of Alloys & Compounds, 2014, 613(7): 139–142.

[4] STYLES M J, HUTCHINSON C R, CHEN Y, DESCHAMPS A, BASTOW T J. The coexistence of two S(Al_2CuMg) phases in Al–Cu–Mg alloys [J]. Acta Materialia, 2012, 60(20): 6940–6951.

[5] LIU J, BRAY G H, LUKASAK D A, PAHL R C. Aluminum alloy extrusions having a substantially unrecrystallized structure: US, US6918975 [P]. 2005.

[6] LI J X, ZHAI T, GARRATT M D, BRAY G H. Four-point-bend fatigue of AA 2026 aluminum alloys [J]. Metallurgical & Materials Transactions A, 2005, 36(9): 2529–2539.

[7] LAM D F, MENZEMER C C, SRIVATSAN T S. A study to evaluate and understand the response of aluminum alloy 2026 subjected to tensile deformation [J]. Materials & Design, 2010, 31(1): 166–175.

[8] LIU Can, ZHANG Hui, JIANG Fu-lin. Characterization of dynamic microstructure evolution during hot deformation of Al–4.10Cu–1.42Mg–0.57Mn–0.12Zr alloy [J]. Transactions of Nonferrous Metals Society of China, 2014, 24(11): 3477–3485.

[9] LIU Xiao-yan, PAN Qing-lin, FAN Xi, HE Yun-bin, LI Wen-bin, LIANG Wen-jie. Microstructural evolution of Al–Cu–Mg–Ag alloy during homogenization [J]. Journal of Alloys & Compounds, 2009, 484: 790–794.

[10] CONG Fu-guan, ZHAO Gang, JIANG Feng, TIAN Ni, LI Rui-feng. Effect of homogenization treatment on microstructure and mechanical properties of DC cast 7X50 aluminum alloy [J]. Transactions of Nonferrous Metals Society of China, 2015, 25(4): 1027–1034.

[11] WANG Hai-jun, XU Ju, KANG Yong-lin, TANG Meng-ou, ZHANG Zhi-feng. Study on inhomogeneous characteristics and optimize homogenization treatment parameter for large size DC ingots of Al–Zn–Mg–Cu alloys [J]. Journal of Alloys & Compounds, 2014, 585(5): 19–24.

[12] LI Bo, PAN Qing-lin, SHI Yun-jia, LI Chen, YIN Zhi-min. Microstructural evolution of Al–Zn–Mg–Zr alloy with trace amount of Sc during homogenization treatment [J]. Transactions of Nonferrous Metals Society of China, 2013, 23(12): 3568–3574.

[13] JIANG Hai-chun, YE Ling-ying, ZHANG Xin-ming, GU Gang, ZHANG Pan, WU Yu-long. Intermetallic phase evolution of 5059 aluminum alloy during homogenization [J]. Transactions of Nonferrous Metals Society of China, 2013, 23(12): 3553–3560.

[14] LI Hong-ying, SU Xiong-jie, YIN Hao, HUANG De-sheng. Microstructural evolution during homogenization of Al-Cu-Li-Mn-Zr-Ti alloy [J]. Transactions of Nonferrous Metals Society of China, 2013, 23(9): 2543–2550.

[15] SHI Yun-jia, PAN Qing-lin, LI Meng-jia, LIU Zhi-ming, HUANG Zhi-qi. Microstructural evolution during homogenization of DC cast 7085 aluminum alloy [J]. Transactions of Nonferrous Metals Society of China, 2015,

25(11): 3560–3568.
[16] DENG Ying, YIN Zhi-min, CONG Fu-guan. Intermetallic phase evolution of 7050 aluminum alloy during homogenization [J]. Intermetallics, 2012, 26(7): 114–121.
[17] LIU Qing, ZHU Rui-hua, LI Jin-fen, CHEN Yong-lai, ZHANG Xu-hu, ZHANG Long, ZHENG Zi-qiao. Microstructural evolution of Mg, Ag and Zn micro-alloyed Al-Cu-Li alloy during homogenization [J]. Transactions of Nonferrous Metals Society of China, 2016, 26(3): 607–619.
[18] GARRATT M D, BRAY G H. The grain boundary geometry for optimum resistance to growth of short fatigue cracks in high strength Al-alloys [J]. International Journal of Fatigue, 2005, 27(s10–12): 1202–1209.
[19] ZHANG Hui, CHEN Rong, HUANG Xu-dong, CHEN Jiang-hua. Microstructural evolution of 2026 aluminum alloy during hot compression and subsequent heat treatment [J]. Transactions of Nonferrous Metals Society of China, 2011, 21(5): 955–961.
[20] HUANG Xu-dong, ZHANG Hui, HAN Yi, WU Wen-xiang, CHEN Jiang-hua. Hot deformation behavior of 2026 aluminum alloy during compression at elevated temperature [J]. Materials Science & Engineering A, 2010, 527(3): 485–490.
[21] ZHANG J, HUANG Y N, MAO C, PENG P. Structural, elastic and electronic properties of θ(Al_2Cu) and S(Al_2CuMg) strengthening precipitates in Al–Cu–Mg series alloys: First-principles calculations [J]. Solid State Communications, 2012, 152(23): 2100–2104.
[22] MONDOLFO L F. Aluminum alloys: Structure and properties [J]. Materials Science in Semiconductor Processing, 1976, 31(11): 651–657.
[23] SHEWMON P G. Diffusion in solids [M]. New York: McGraw-Hill, 1963: 61.
[24] LI Wen-bin, PAN Qing-lin, XIAO Yan-ping, HE Yun-bin, LIU Xiao-yan. Microstructural evolution of ultra-high strength Al-Zn-Cu-Mg-Zr alloy containing Sc during homogenization [J]. Transactions of Nonferrous Metals Society of China, 2011, 21(10): 2127–2133.

(Edited by YANG Hua)

中文导读

均匀化处理对 2026 铝合金微观组织的影响

摘要：采用金相分析、扫描电镜、能谱分析、差示扫描量热法以及 X 射线衍射分析等手段，研究均匀化过程中 2026 铝合金微观组织的演变。结果表明：在 2026 合金铸态组织中，出现严重的枝晶偏析现象，晶界处的第二相主要是 S 相(Al_2CuMg)和 θ 相(Al_2Cu)，元素 Cu、Mg 和 Mn 在晶内及晶界分布不均匀。在均匀化过程中，随着均匀化温度的升高或均匀化时间的延长，残留相逐渐溶入基体 α (Al)，元素分布逐渐均匀。综合考虑显微组织演变、差示扫描量热分析和 X 射线衍射分析等，最佳均匀化制度为 490 ℃，24 h，与均匀化动力学分析结果相符合。

关键词：2026 铝合金；枝晶偏析；均匀化；微观组织演变；均匀化动力学